NUCLEAR DEFORMATION EFFECTS IN THE CLUSTER RADIOACTIVITY

Şerban Mişicu

Department of Theoretical Physics, NINPE-HH
Bucharest-Magurele, POB MG-6, Romania
e-mail: misicu@theor1.ifa.ro

and Dan Protopopescu†

Frank Laboratory of Neutron Physics, JINR
141980 Dubna, Moscow Region, Russia

(Received August 25, 1998)

We investigate the influence of the nuclear deformation on the decay rates of some cluster emission processes. The interaction between the daughter and the cluster is given by a double folding potential including quadrupole and hexadecupole deformed densities of both fragments. The nuclear part of the nucleus–nucleus interaction is density dependent and at small distances a repulsive core in the potential will occur. In the frame of the WKB-approximation the assault frequency of the cluster will depend on the geometric properties of the potential pocket whereas the penetrability will be sensitive to changes in the barrier location. The results obtained in this paper point out that various combinations of cluster and daughter deformations may account for the measured values of the decay rate. The decay rates are however more sensitive to the changes in the daughter deformation due to the large mass asymmetry of the process.

PACS numbers: 21.60.Gx, 23.70.+j, 27.90.+b

1. Introduction

The theoretical study of the heavy-cluster emission and the super-asymmetric fission started at the end of seventies [1]. Since the beginning, this phenomenon was recognized to be a consequence of the shell closure of one or both fragments because of its cold nature, *i.e.* the low excitation energy

† On leave of absence from National Institute for Material Physics, Bucharest-Măgurele, POB MG-7, Romania.

involved in the process. Later on, Rose and Jones confirmed experimentally the existence of this new phenomenon [2]. Since then many theoretical and experimental studies have been carried out (for a review see [3]). Recently it was advocated that the cluster radioactivity is not an isolated phenomenon, and must be related to other processes like the cold fusion or cold fission [4], where the closed shell effects play a dominant role. A still opened problem in the study of the cluster radioactivity is represented by the question of the existence of only the spherical or both the spherical and the deformed closed shells. Although both daughter and emitted cluster have in many cases, at least for even-even nuclei, a vanishing quadrupole deformation in the ground state, higher multipole deformations are not rulled out according to liquid drop calculations [5]. Until now there are no experimental data available for deformed daughters.

The influence of the ground-state deformations on the fragment emission probability have been considered in the past [6]. However, the inclusion of the deformation did not destroyed the relative satisfactory agreement already obtained between the experimental results and the results of simple models without deformation. The first theoretical study of the cluster deformation effects on the WKB penetrabilities have been carried out by Săndulescu *et al.* [7] using the double folded Michigan-3 Yukawa (M3Y) potential for a spherical daughter and a quadrupole deformed emitted cluster. The barrier assault frequency ν_0 was depending on the deformation only by means of the first turning point location, such that for a deformed configuration the barrier was shifted at a larger interfragment distance and ν_0 was decreasing.

In this paper we extend the study of the deformation effects in cluster radioactivity by accounting also for the deformation of the daughter nucleus and including higher multipole deformations, like the hexadecupole one. The interaction between the daughter nucleus and the cluster, in the region of small overlap and throughout the barrier is computed by means of a double folding potential. The nuclear part includes a repulsive core at small distances. In this way our deformed cluster approach supposes a cluster already formed in the potential pocket coming from the interplay between the Coulomb and the repulsive nuclear core on one hand and the attractive nuclear force on the other hand. The depth and the width of this pocket will determine the assault frequency of the cluster on the barrier, through which it will eventually tunelate. In its turn, the penetrability will depend on the height and width of the barrier. Since all these geometrical characteristics depend sensitively on the shape of the fragments we will investigate in this paper the modification induced by the quadrupole and hexadecupole deformations of the fragments on the pocket and the barrier and finally compute decay rates for several cluster emitters.

2. Cluster–daughter double-folding potential

The nuclear interaction between the daughter and the cluster can be calculated as the double folding integral of ground state one-body densities $\rho_{1(2)}(\boldsymbol{r})$ of heavy ions as follows

$$U_N(\boldsymbol{R}) = \int d\boldsymbol{r}_1 d\boldsymbol{r}_2 \ \rho_1(\boldsymbol{r}_1)\rho_2(\boldsymbol{r}_2)v(\boldsymbol{s})\,, \tag{2.1}$$

where v is the NN effective interaction and the separation distance between two interacting nucleons is denoted by $\boldsymbol{s} = \boldsymbol{r}_1 + \boldsymbol{R} - \boldsymbol{r}_2$, R being the centre-to-centre distance. In the past a G-matrix M3Y effective interaction was used to discuss light and heavy cluster radioactivity [7,8]. This interaction contains isoscalar and isovector Yukawa functions in each spin-isospin (S,T) channel and an exchange component coming from the one-nucleon knock-on exchange term. However, this interaction is based on density-independent nucleon-nucleon forces and consequently very deep nucleus–nucleus potentials are obtained. A double folding potential based on the effective Skyrme interaction will contain a repulsive core which would prevent, according to the Pauli principle, a large overlap of the two interacting nuclei [9]. Thus the nuclear potential between two ions contains an attractive part and a repulsive one. Neglecting the spin dependence, it can be written as

$$U_N(\boldsymbol{R}) = C_0 \left\{ \frac{F_{\rm in} - F_{\rm ex}}{\rho_{00}} \left((\rho_1^2 * \rho_2)(\boldsymbol{R}) + (\rho_1 * \rho_2^2)(\boldsymbol{R}) \right) + F_{\rm ex}(\rho_1 * \rho_2)(\boldsymbol{R}) \right\}, \tag{2.2}$$

where $*$ denotes the convolution of two functions f and g, *i.e.* $(f * g)(\boldsymbol{x}) = \int f(\boldsymbol{x}')g(\boldsymbol{x} - \boldsymbol{x}')d\boldsymbol{x}'$. The constant C_0 and the dimensionless parameters $F_{\rm in}, F_{\rm ex}$ are given in Ref. [9]. To solve this integral we consider the inverse Fourier transform

$$U_N(\boldsymbol{R}) = \int \mathrm{e}^{-i\boldsymbol{q}\cdot\boldsymbol{R}} \widetilde{U}_N(\boldsymbol{q}) d\boldsymbol{q}\,, \tag{2.3}$$

where the Fourier transform of the local Skyrme potential $\widetilde{U}_N(\boldsymbol{q})$ can be casted in the form

$$\widetilde{U}_N(\boldsymbol{q}) = C_0 \left\{ \frac{F_{\rm in} - F_{\rm ex}}{\rho_{00}} \left(\widetilde{\rho_1^2}(\boldsymbol{q})\widetilde{\rho}_2(-\boldsymbol{q}) + \widetilde{\rho}_1(\boldsymbol{q})\widetilde{\rho_2^2}(-\boldsymbol{q}) \right) + F_{\rm ex}\widetilde{\rho}_1(\boldsymbol{q})\widetilde{\rho}_2(\boldsymbol{q}) \right\}. \tag{2.4}$$

Here $\widetilde{\rho}(\boldsymbol{q})$ and $\widetilde{\rho^2}(\boldsymbol{q})$ are Fourier transforms of the nucleon densities $\rho(\boldsymbol{r})$ and squared nuclear densities $\rho^2(\boldsymbol{r})$. Expanding the nucleon densities for axial-symmetric distributions in spherical harmonics we get

$$\rho(\boldsymbol{r}) = \sum_{\lambda} \rho(r) Y_{\lambda 0}(\theta, 0)\,. \tag{2.5}$$

Then

$$\widetilde{\rho}(\boldsymbol{q}) = 4\pi \sum_{\lambda} i^{\lambda} Y_{\lambda 0}(\theta_q, 0) \int_0^{\infty} r^2 dr \rho_{\lambda}(r) j_{\lambda}(qr)\,, \tag{2.6}$$

$$\widetilde{\rho^2}(\boldsymbol{q}) = \sqrt{4\pi} \sum_{\lambda} \frac{i^{\lambda}}{\hat{\lambda}} Y_{\lambda 0}(\theta_q, 0) \sum_{\lambda' \lambda''} \hat{\lambda}' \hat{\lambda}'' (C^{\lambda \lambda' \lambda''}_{0\,0\,0})^2 \times \int_0^{\infty} r^2 dr \rho_{\lambda'}(r) \rho_{\lambda''}(r) j_{\lambda}(qr)\,. \tag{2.7}$$

In this paper we take the one-body densities for both daughter and cluster as two-parameter Fermi distributions in the intrinsic frame for axial symmetric nuclei

$$\rho(\boldsymbol{r}) = \frac{\rho_{00}}{1 + \exp((r - R(\theta))/a)}\,. \tag{2.8}$$

Here $\rho_{00} = 0.17\,\mathrm{fm}^{-3}$, a denotes the diffusivity which is taken to be 0.63 fm for the daughter and 0.67 fm for the cluster, and

$$R(\theta) = R_0 \left(1 + \beta_2 \sqrt{\frac{5}{4\pi}} P_2(\cos\theta) + \beta_4 \frac{3}{\sqrt{4\pi}} P_4(\cos\theta)\right) \tag{2.9}$$

is the parameterization of the nuclear shape in quadrupole β_2 and hexadecupole β_4 deformations. Here $R_0 = r_0 A^{1/3}$ with r_0 computed by means of a liquid drop prescription [5].

3. Calculus of decay constants

We adopt a modified Gammow approach [3] which is based on the idea that the cluster is pre-born, with a certain probability P_0, in the pocket of the Skyrme+Coulomb potential and later on it tunnels through an essentially one-dimensional barrier. Although in the present case, having deformed fragments, we deal with a multi-dimensional penetration problem, we can disregard the orientation effects in a first approximation. It is not difficult to show that the value of the penetrability is maximized on the fission path corresponding to daughter and cluster having their symmetry axes oriented along the inter-fragment axis. For such a configuration the top of the barrier will attain a minimum and its location is found at a larger interfragment distance.

Consequently the decay rate λ will be defined as follows:

$$\lambda = \nu_0 P_0 P\,, \tag{3.1}$$

where ν_0 is the assault frequency with which the cluster bombards the walls of the potential pocket. It is given by the inverse of the classical period of motion

$$T_0 = \int_{r_{t1}}^{r_{t2}} dr \sqrt{\frac{2\mu}{Q - V(r)}}, \tag{3.2}$$

where μ is the reduced mass of the cluster-daughter pair and r_{t1} and r_{t2} are the inner turning points, where the potential curve intersects the Q-value (see Fig. 1). Thus, in our model, ν_0 depends sensitively on the size of the potential pocket. The barrier penetrability is computed in the frame of the WKB approach

$$P = \exp\left(-2 \int_{r_{t2}}^{r_{t3}} dr \sqrt{\frac{2\mu}{\hbar^2}(U(r) - Q)}\right), \tag{3.3}$$

where r_{t3} is the outer turning point.

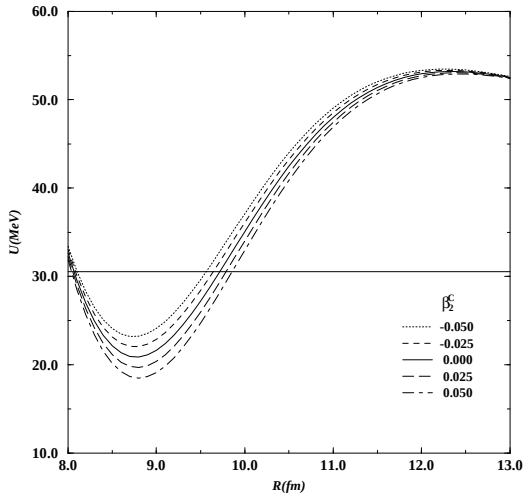

Fig. 1. Variation of the interaction potential $U(R)$ with the quadrupole deformation of the cluster, β_2^{C}, when the ground hexadecupole deformation for ^{210}Pb is kept fixed, $\beta_4^{\mathrm{D}} = 0.008$. The distance R is measured between the centers of mass of the two nuclei. The horizontal line at 30.53 MeV is the Q-value of the decay.

The calculus of the preformation probability P_0 is usually based on elaborated microscopic models. Since its calculation is beyond the purpose of this paper, we limit ourselves to a simple empirical formula proposed by

Blendowske *et al.* [10] for light clusters

$$P_0 = (P_0^\alpha)^{\frac{A_c-1}{3}} \qquad (A_c \leq 28)\,, \tag{3.4}$$

where the subscript c refers to the cluster and the α-spectroscopic factor is estimated as

$$(P_0^\alpha)^{\text{even}} = 6.3 \times 10^{-3} \qquad \text{and} \qquad (P_0^\alpha)^{\text{odd}} = 3.2 \times 10^{-3}\,. \tag{3.5}$$

In what follows we consider the ^{14}C-decay of ^{224}Ra.

In Fig. 1 we plotted a family of potential curves $U(R)$ for several quadrupole deformations β_2^{C} of the cluster ^{14}C and a fixed hexadecupole deformation of the daughter, chosen to be $\beta_4^{\text{D}} = 0.008$, *i.e.* the ground state value for ^{210}Pb. As one can see on this plot, the increase of β_2^{C} from negative to positive values is accompanied by the lowering of the barrier, while the bottom of the pocket goes down further. The decay rate is influenced mainly by the changes with deformation in the region between the first turning point and the top of the barrier.

For comparison, the next plot, Fig. 2, shows the variation of the interaction potential with the hexadecupole deformation of the cluster. The variation brought by the hexadecupole deformation is slightly different. Like in the previous case, the barrier lowers with β_4^{C}, but the bottom of the pocket rises. Obviously, this will affect the values of life-times in a different way than the one β_2^{C} does. The assault frequency ν_0 will decrease with increasing cluster hexadecupole deformation, but not enough to compensate the increase of penetrability. In overall the decay rate will increase with β_4^{C} slower than with β_2^{C}.

Plots of the interaction potential $U(R)$ for different pairs $(\beta_2^{\text{D}};\beta_2^{\text{C}})$ of quadrupole deformation are shown in Fig. 3. One can compare the magnitude of the effect of both cluster and daughter quadrupole deformations and the changes which occur when we pass from prolate to oblate deformation. One can notice that the quadrupole deformation β_2^{C} of the cluster acts mainly on the right wall of the pocket, while the modification of the quadrupole deformation of the daughter nucleus pushes in opposite directions both walls of the pocket.

The difference between positive and negative quadrupole and hexadecupole deformations of the daughter nucleus can be easily understood from Fig. 4. We observe different type of modifications in the shape of the pocket, corresponding to β_2 and β_4 deformations, respectively. The quadrupole and hexadecupole deformations of the daughter change the depth of the potential pocket in the same manner, in comparison with the case of cluster deformations which, as we saw in figures 1 and 2, move the bottom of the pocket in opposite directions.

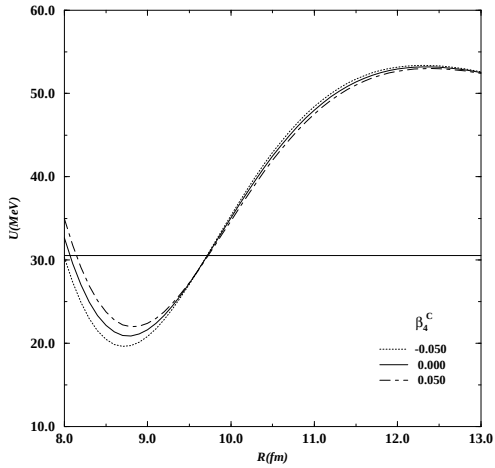

Fig. 2. Variation of the interaction potential $U(R)$ with the hexadecupole deformation of the cluster, $\beta_4^{\rm C}$. All deformation parameters, except $\beta_4^{\rm D}$=0.008, are zero.

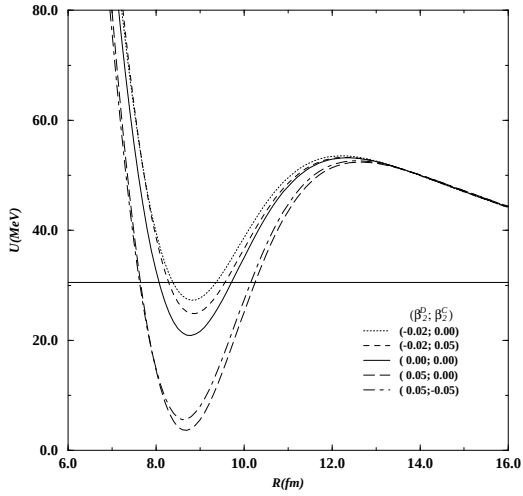

Fig. 3. Plots of the interaction potential $U(R)$ for different pairs of daughter–cluster quadrupole deformation ($\beta_2^{\rm D}$;$\beta_2^{\rm C}$).

A plot of calculated λ, as a function of the hexadecupole deformation of the daughter nucleus $\beta_4^{\rm D}$, for several values of $\beta_2^{\rm D}$ and a spherical cluster, is drawn in logarithmic scale in Fig. 5. One can see, for example, that if the daughter nucleus has no quadrupole deformation a hexadecupole deformation $\beta_4^{\rm D} \approx 0.04$ may account for the experimental decay rate. Values of the decay rate close to the experimental one can be attained also by combina-

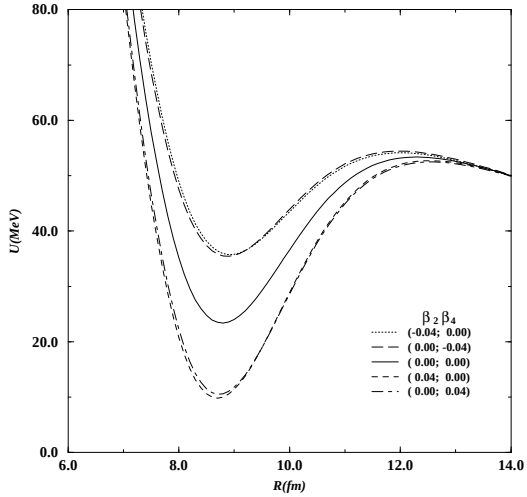

Fig. 4. Comparison between the effects of quadrupole and hexadecupole deformations of the daughter nuclei. Here, contrary to the case when the cluster is deformed, the quadrupole and hexadecupole deformations modify the depth of the pocket in the same manner.

tions of non-vanishing quadrupole and hexadecupole deformations.

The next figure presents the variation of the calculated decay rate λ with cluster hexadecupole deformation for four fixed values of β_2^{C} (see Fig. 6). This time the daughter nucleus is taken to be spherical. Recalling the observations made earlier, in connection with figures 1 and 2, on the modification of the potential due to the quadrupole and hexadecupole deformations one may understand why λ increases faster with β_4^{D} than with β_4^{C}. Therefore, one may infer that it is less favorable to emit the daughter with a non-zero hexadecupole deformation.

In Table I we selected some of the most favorable cases for the calculated decay rates of several cluster decay reactions. As we expected, prolate deformations favor the decay. In the case of ^{14}C decay of ^{224}Ra deformations between -0.04 and 0.04 in β_2^{D} give us decay rates which match the experimental one provided β_4^{D} is taken to be not to large compared to the ground state value, *i.e.* 0.008. We may also consider a case when the cluster is deformed and the daughter is spherical. In the case of ^{14}C decay of ^{226}Ra, a hexadecupole deformation, not too larger than its ground state value, still accounts for the experimental value although all other deformations are zero.

The fact that the decay rates are more sensitive to the daughter deformations can be easily understood on ground of the mass asymmetry of the decaying system. An easy to follow explanation of this fact is given

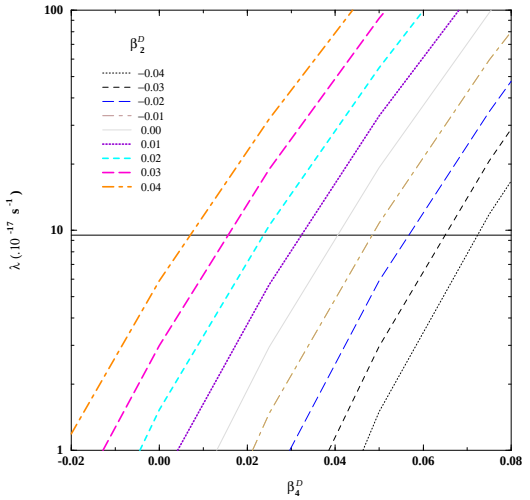

Fig. 5. The dependency of λ on β_4^{D} in logarithmic scale for several values of quadrupole deformation of the daughter nucleus. The cluster is spherical in all cases. The horizontal line represents the experimental value for the discussed decay, $\lambda_{\mathrm{exp}} = 9.50 \times 10^{-17}\ \mathrm{s}^{-1}$.

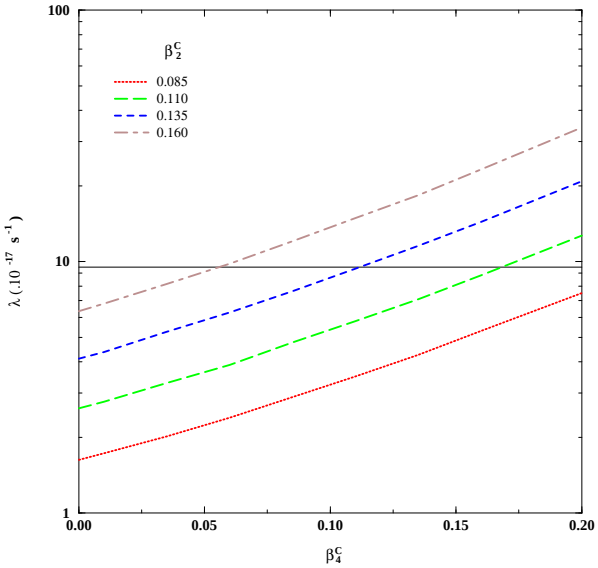

Fig. 6. Plots of the variation of calculated decay rate λ with hexadecupole deformation of cluster for four fixed values of β_2^{C}. The daughter nucleus is taken spherical.

TABLE I

Deformations of clusters and daughters which fit the calculated decay rate (see Eq. (3.1)) to the experimental one $\lambda_{\rm exp}$. Empty spaces in the table mean null values.

Decay	Cluster		Daughter		$\lambda_{\rm exp}$
	$\beta_2^{\rm C}$	$\beta_4^{\rm C}$	$\beta_2^{\rm D}$	$\beta_4^{\rm D}$	(s^{-1})
$^{224}Ra \rightarrow {}^{14}C + {}^{210}Pb$	0.160	0.056			$9.50 \cdot 10^{-17}$
			-0.040	0.072	
				0.040	
			0.040	0.007	
$^{226}Ra \rightarrow {}^{14}C + {}^{212}Pb$				0.029	$3.50 \cdot 10^{-22}$
$^{234}U \rightarrow {}^{24}Ne + {}^{210}Pb$	-0.215	0.155		0.098	$5.94 \cdot 10^{-26}$
	0.170			0.010	
$^{234}U \rightarrow {}^{28}Mg + {}^{206}Hg$	0.323	-0.136	-0.033		$2.00 \cdot 10^{-26}$
	0.113		0.080	0.080	
$^{230}Th \rightarrow {}^{24}Ne + {}^{206}Hg$	-0.215	0.155	0.123		$1.60 \cdot 10^{-25}$
			0.063		

if we consider only the Coulomb part of the barrier. The asymptotic part of the barrier, including the region where the third turning point r_{t_3} is located, is determined essentially by the Coulomb multipoles. Introducing the quadrupole moments of the charge density

$$Q_2^{\rm D,C} = \sqrt{\frac{4\pi}{5}} \int_0^\infty r^2 dr \rho_2^{\rm D,C}(r) r^2 \tag{3.6}$$

the potential will behave for $R \to \infty$ as

$$(C_{000}^{202})^2 \frac{Z_{\rm C} Q_2^{\rm D} + Z_D Q_2^{\rm C}}{R^3}. \tag{3.7}$$

Since the quadrupole moments of the daughter $Q_2^{\rm D}$ and cluster $Q_2^{\rm C}$ depend on their quadrupole deformations β_2 it is obvious that due to the asymmetry in mass and charge ($Z_{\rm C}/Z_{\rm D} \approx 0.1$), the deformation of the daughter will have a larger influence on the barrier and eventually on the value of the decay rate.

4. Conclusions

The aim of this paper was to extend previous studies of deformation effects in cluster radioactivity by considering also the deformation of the

daughter nucleus and to include the next higher even deformation, the hexadecupole one. Considering that the cluster is pre-born in the potential pocket produced by the interplay between repulsive and attractive forces, we investigated the modifications induced by deformations on the specific potential that we employ. The computed decay rates depend on the assault frequency, which varies with the pocket depth, and on the penetrability, which changes with the barrier height. We showed that the experimental values can be reproduced for several selections of the deformations. If we maintain the cluster spherical and vary the quadrupole and/or hexadecupole deformations of the daughter nucleus we may reach the experimental value within a reasonable range of deformations parameters. Conversely, if the daughter is spherical, then only for significant values of β_2^{C} we can reproduce the experimental value without taking into account β_4^{C}. One might conclude that deformed states of the daughter are needed to be considered in order to reach the experimental λ within reasonable values of cluster deformation. Configurations with a spherical cluster and only a hexadecupole deformation for the daughter are likely to occur. Also combinations of small deformations of both fragments should not be discarded. In conclusion, the study carried out in this paper points mainly to the importance of the daughter nucleus deformations, and especially its hexadecupole one.

One of the authors (Ş.M.) would like to acknowledge the hospitality of Prof. R. Jolos at the Bogoliubov Laboratory for Theoretical Physics during the completion of this work and to express its gratitude to Dr. A. Nasirov for many enlightening discussions. We are also very indebted to Dr. F. Cârstoiou who provided us with the routines for calculating the Coulomb part of the interaction potential.

REFERENCES

[1] A. Săndulescu, D.N. Poenaru, W. Greiner, *Sov. J. Part. Nucl.* **11**, 528 (1980).

[2] H.J. Rose, G.A. Jones, *Nature* **307**, 245 (1984).

[3] R.K. Gupta, W. Greiner, *Int. J. Mod. Phys.* **3**, 335 (1994).

[4] A. Săndulescu, A. Florescu, W. Greiner, *J. Phys. G: Nucl. Part. Phys.* **15**, 1815 (1989); S. Singh, R.K. Gupta, W. Scheid, W. Greiner, *J. Phys. G: Nucl. Part. Phys.* **18** , 1243 (1992).

[5] P. Möller, J.R. Nix, W.D. Myers, W.J. Swiatecki, *At. Data Nucl. Data Tables* **59**, 185 (1995).

[6] Y.J. Shi, W.J. Swiatecki, *Nucl. Phys.* **464**, (1987) 205.

[7] A. Săndulescu, R.K. Gupta, F. Cârstoiu, M. Horoi, W. Greiner, *Int. J. Mod. Phys.* **E1**, 379 (1992); R.K. Gupta, M. Horoi, A. Săndulescu, M. Greiner, W. Scheid, *J. Phys. G: Nucl. Part. Phys.* **19**, 2063 (1993).

[8] A. Săndulescu, Ş. Mişicu, F. Cârstoiu, A. Florescu, W. Greiner, *Phys. Rev.* **C57**, 2321 (1998).

[9] G.G. Adamian, N.V. Antonenko, R.V. Jolos, S.P. Ivanova, O.I. Melnikova, *Int. J. Mod. Phys.* **E5**, 191 (1996).

[10] R. Blendowske, T. Fliessbach, H. Walisser, *Z. Phys.* **A339**, 191 (1991).